

CERN LIBRARIES, GENEVA



SCAN-9704055

Swg715

IPNO DRE 97-08

**Proton Scattering on the Unstable  $^{38}\text{S}$  Nucleus : Isovector  
Contribution to the  $2_1^+$  State**

J. H. Kelley<sup>1,\*</sup>, T. Suomijärvi<sup>1,2</sup>, S. E. Hirzebruch<sup>1,2</sup>, A. Azhari<sup>2,3,†</sup>,  
D. Bazin<sup>2</sup>, Y. Blumenfeld<sup>1</sup>, J. A. Brown<sup>2,‡</sup>, P. D. Cottle<sup>4</sup>, S.  
Danczyk<sup>2,3</sup>, M. Fauerbach<sup>2,3</sup>, T. Glasmacher<sup>2,3</sup>, J. K. Jewell<sup>4</sup>, K.  
W. Kemper<sup>4</sup>, F. Maréchal<sup>1</sup>, D. J. Morrissey<sup>2,5</sup>, S. Ottini<sup>6</sup>, J. A.  
Scarpaci<sup>1</sup>, and P. Thirolf<sup>2,§</sup>

<sup>1</sup>*Institut de Physique Nucléaire, IN2P3-CNRS, 91406 Orsay, France*

<sup>2</sup>*NSCL/MSU, East Lansing, MI 48824, USA*

<sup>3</sup>*Depart. of Physics and Astronomy, MSU, East Lansing, MI 48824, USA*

<sup>4</sup>*Department of Physics, FSU, Tallahassee, FL 32306, USA*

<sup>5</sup>*Department of Chemistry, MSU, East Lansing, MI 48824, USA*

<sup>6</sup>*SEPhN, DAPNIA, CEA Saclay, 91191 Gif sur Yvette, France*

# Proton Scattering on the Unstable $^{38}\text{S}$ Nucleus : Isovector Contribution to the $2_1^+$ State

J. H. Kelley<sup>1,\*</sup>, T. Suomijärvi<sup>1,2</sup>, S. E. Hirzebruch<sup>1,2</sup>, A. Azhari<sup>2,3,†</sup>, D. Bazin<sup>2</sup>, Y. Blumenfeld<sup>1</sup>, J. A. Brown<sup>2,‡</sup>, P. D. Cottle<sup>4</sup>, S. Danczyk<sup>2,3</sup>, M. Fauerbach<sup>2,3</sup>, T. Glasmacher<sup>2,3</sup>, J. K. Jewell<sup>4</sup>, K. W. Kemper<sup>4</sup>, F. Maréchal<sup>1</sup>, D. J. Morrissey<sup>2,5</sup>, S. Ottini<sup>6</sup>,  
J. A. Scarpaci<sup>1</sup> and P. Thirolf<sup>2,§</sup>

<sup>1</sup> *Institut de Physique Nucléaire, IN2P3-CNRS, 91406 Orsay, France*

<sup>2</sup> *National Superconducting Cyclotron Laboratory, Michigan State University, East Lansing, MI 48824*

<sup>3</sup> *Department of Physics and Astronomy, Michigan State University, East Lansing, MI 48824*

<sup>4</sup> *Department of Physics, Florida State University, Tallahassee, FL 32306*

<sup>5</sup> *Department of Chemistry, Michigan State University, East Lansing, MI 48824*

<sup>6</sup> *SEPhN, DAPNIA, CEA Saclay, 91191 Gif sur Yvette, France*

## Abstract

A 39A MeV  $^{38}\text{S}$  radioactive beam was used with inverse kinematics to measure angular distributions for elastic and inelastic proton scattering from a  $\text{CH}_2$  target. Optical potential and folding model calculations are compared with the elastic distribution. Using coupled channel calculations, the  $\beta_2$  value for the  $2_1^+$  state is determined to be  $0.35 \pm 0.04$ . This value, when compared with the corresponding result from a Coulomb excitation measurement, leads to  $M_n/M_p = (1.5 \pm 0.3) N/Z$ , indicating an isovector contribution to the  $2_1^+$  state of  $^{38}\text{S}$ .

PACS numbers: 21.10.Re, 25.40.Cm, 25.40.Ep, 25.60.-t

Typeset using REVTeX

Nuclei are generally treated as having an inert closed shell core coupled to valence protons and neutrons, which primarily determine the nuclear structure. However, evidence suggests that the "magic number" shell closures do not always persist in nuclei outside the valley of stability. Therefore it is of paramount importance to investigate the evolution of nuclear structure when moving towards the drip lines. The use of multiple experimental probes allows us to disentangle the effects due to protons and neutrons in the nucleus.

Great current interest is focused on neutron rich nuclei near the  $N=28$  magic number for which theoretical calculations predict the onset of deformation [1,2]. Advances in beam currents available at a number of radioactive nuclear beam facilities have recently extended the region of nuclei accessible for direct study. In the  $N=28$  region,  $\beta$ -decay measurements of the nuclei  $^{43}\text{P}$ ,  $^{44}\text{S}$  and  $^{45}\text{Cl}$  indicate deformation in these neutron "magic number" nuclei [3]. The excitation energy and  $B(E2)$  values of the  $2_1^+$  states in  $^{38,40,42,44}\text{S}$  [2,4] have been measured through Coulomb excitation. The  $B(E2)$  values show evidence of deformation beginning in  $^{40}\text{S}$ .

More detailed information on nuclear structure can be revealed through elastic and inelastic proton scattering. Low lying  $2^+$  and  $3^-$  states are generally well represented by an isoscalar collective model with equal neutron and proton deformation, yielding a ratio of the neutron and proton multipole transition matrix elements  $M_n/M_p = N/Z$  [5]. However, comparisons of transition probabilities measured with different probes have been used to detect deviations from the simple isoscalar picture, particularly in single closed shell nuclei, where the valence nucleons drive the oscillations [6]. In this sense, an experimental determination of  $M_n/M_p$  gives indications about the nature of the excitation and about shell structure effects. At energies of a few tens of MeV, inelastic proton scattering is mostly sensitive to the neutrons in the nucleus, and is therefore a very suitable tool to determine  $M_n/M_p$  by a comparison with the deformation parameter obtained from electromagnetic excitation, which is only sensitive to the protons [5].

Since the advent of radioactive beam facilities, it has become possible to measure proton scattering on short lived nuclei in inverse kinematics, using a proton target. Reaction

kinematics are then determined either by detecting the heavy ejectile or recoiling protons. Such studies are restricted to nuclei closer to the valley of stability than half-life or Coulomb excitation measurements, since the prerequisite of very thin targets, which preserve the kinematic characteristics of the outgoing particles, requires the availability of sizeable beam currents, at least several  $10^3$  particles per second. Earlier proton scattering experiments with unstable beams have mainly involved light unstable nuclei. An exception is the doubly magic nucleus  $^{56}\text{Ni}$  which was studied by (p,p') scattering in inverse kinematics at 101A MeV [7]. In this study, the  $\beta_2$ -value was extracted from cross section measurements at only one scattering angle. Up to now, angular distributions of inelastic scattering on unstable nuclei produced by projectile fragmentation have not been reported.

This letter presents results of elastic and inelastic proton scattering on  $^{38}\text{S}$  in inverse kinematics, measured over a broad angular range, using large solid-angle position sensitive detectors to measure recoiling protons. The value of  $\beta_2$  is extracted for the  $2_1^+$  state, and from a comparison with a Coulomb excitation measurement, the first experimental  $M_n/M_p$  value for the excited state of a short lived nucleus is extracted.

A beam of 85A MeV  $^{40}\text{Ar}$  nuclei, provided by the K1200 cyclotron at the National Superconducting Cyclotron Laboratory, impinged on a  $376\text{ mg/cm}^2$  Be target located at the production target position of the A1200 fragment separator [8]. The resulting beam was purified by using a  $292\text{ mg/cm}^2$  aluminum wedge, and limited to a momentum spread of  $\Delta p/p = 1\%$ , yielding a  $^{38}\text{S}$  beam that was more than 99% pure.

The beam, consisting of around  $2 \times 10^5$  particles per second, was then collimated sufficiently ( $\Delta\theta_{beam} \leq 0.3^\circ$  FWHM) so that it was unnecessary to carry out event-by-event trajectory tracing. The final beam intensity was around  $3 \times 10^4$  particles per second. A  $1.9\text{ mg/cm}^2$   $\text{CH}_2$  target was rotated to an angle of  $34^\circ$  with respect to the beam direction, thus providing an effective in beam target thickness of  $4.6\text{ mg/cm}^2$ , while limiting the energy loss and angular straggling of low energy protons recoiling towards the detectors. A  $0^\circ$ -detector, placed downstream from the target, consisted of a thin and thick fast plastic. This detector covered scattering angles up to  $4.7^\circ$ , largely above the kinematic limit for elas-

tic and inelastic scattering of  $^{38}\text{S}$  from protons, and provided a  $\Delta E$ - $E$  separation of heavy projectile-like fragments from lighter reaction products, a scaler count of the  $^{38}\text{S}$  particle flux, and a time signal.

A group of 5 telescopes,  $5 \times 5$  cm active area, consisting of a  $300\mu\text{m}$  thick Si strip detector followed by a second  $300\mu\text{m}$  or  $500\mu\text{m}$  thick Si detector and a 1 cm thick stopping CsI, were positioned 29 cm from the target to measure recoiling protons. The telescopes covered laboratory angles between  $62^\circ$  and  $88^\circ$ . The first Si detector was segmented into 16 vertical strips (3.125 mm spacing or  $0.6^\circ$  in the lab frame). An energy signal and a time signal stopped by the  $0^\circ$   $\Delta E$  plastic detector was read for each strip and identified particles stopping in these detectors. The time resolution was  $\sim 900$  ps FWHM for 3.2 MeV protons. Higher energy particles that punched through the first detector, were identified by their  $\Delta E$ - $E$  signal in Si-Si or Si-CsI.

Scattered protons were selected with a requirement that a heavy ejectile must survive the collision and be detected in the  $0^\circ$   $\Delta E$ - $E$  plastic stopping detector. The laboratory angle of the scattered protons was determined from the strip detector. After randomizing by software the position of protons evenly across the surface of a given strip, the center of mass (CM) angle and  $^{38}\text{S}$  excitation energy were calculated on an event by event basis.

Before measuring the  $^{38}\text{S}$  scattering, the experimental method was tested with the  $^{40}\text{Ar}$  beam degraded to 40A MeV. Figure 1(a) shows an energy vs. laboratory angle scatterplot for recoiling protons scattered by the  $^{40}\text{Ar}$  beam. The observed kinematic lines correspond to the ground state and first  $2^+$  and  $3^-$  states of  $^{40}\text{Ar}$ . The insert in Fig.1(a) shows the excitation energy spectrum for the angular bin between  $30.5^\circ$  and  $31.5^\circ$  in the CM frame. The overall angular resolutions were on the order of  $1.6^\circ$  FWHM in the laboratory frame and  $3.2^\circ$  FWHM in the CM frame. The primary source of angular uncertainty came from the angular acceptance introduced by the 3.1 mm strip size and the  $\sim 4$  mm FWHM beam spot size. The excitation energy resolution, which depends largely on the laboratory angular resolution, varies from around 600 keV at low CM angles to 900 keV at higher CM angles. Because of the high beam intensity available for  $^{40}\text{Ar}$ , the  $0^\circ$   $\Delta E$ - $E$  plastic detector was

not used to measure coincident projectile-like fragments. This leads to a large background, presumably resulting from central collisions of  $^{40}\text{Ar}$  on protons and  $^{12}\text{C}$ , and also precludes obtaining an absolute normalization. The ratio of elastic scattering to inelastic scattering to the  $2_1^+$  state was obtained from a gaussian fit to the spectrum, after background subtraction. The deformation parameter  $\beta_2$  was extracted for the  $2_1^+$  state by comparing the measured ratio to a coupled channel calculation performed with the code ECIS [9] using optical model parameters from ref. [10]. This yields  $\beta_2=0.29\pm 0.03$  for  $^{40}\text{Ar}$ ; which is slightly larger but consistent with the previous measurements of 0.24-0.26 [11], in spite of the large background.

In the case of  $^{38}\text{S}$ , the  $2_1^+$  state is known to be located at 1.29 MeV [12]. Figure 1(b) displays a scatterplot of laboratory energy vs. angle for recoiling protons from the  $^{38}\text{S}$  scattering. Despite lower statistics than in the  $^{40}\text{Ar}$  test case, elastic scattering and inelastic scattering to a state at 1.2 MeV, which can be identified as the  $2_1^+$  state, are clearly separated. Indications for the presence of higher lying states are also observed. The insert shows the excitation energy spectrum for an angular bin between  $27^\circ$  and  $30^\circ$  in the CM frame. Note that in the case of the 39A MeV  $^{38}\text{S}$  beam, the background is strongly suppressed by requiring that a heavy ejectile be observed in the  $0^\circ$   $\Delta E$ -E detector in coincidence with scattered protons. The use of the  $0^\circ$ -detector also allowed an absolute normalization of the data, and the identification of protons down to about 1 MeV through their time of flight measurement. The energy and angular resolutions are similar to those obtained in the  $^{40}\text{Ar}$  test case.

The elastic scattering angular distribution of  $^{38}\text{S}$ , Fig. 2(a), is obtained by projecting the contents of a contour in the excitation energy vs.  $\theta_{CM}$  plane. Above  $\theta_{CM}=40^\circ$  the ground state and  $2_1^+$  state are not resolved, and in this range the predicted cross section for the  $2_1^+$  state (with the  $\beta_2$  value obtained below), which amounts to about 10% of the elastic cross section, was subtracted from the measured quasielastic distribution.

Coupled-channels predictions using the ECIS code [9] are shown in comparison with the data. Note that no arbitrary normalization is involved here. A calculation based on the Becchetti-Greenlees parameterization [13], which was developed for (p,p) scattering on

$A \geq 40$  nuclei, is shown by the dashed line in Fig. 2. A second calculation, shown as the solid line in Fig. 2, uses optical model parameters for  $^{40}\text{Ar}(p,p)$  [10] and gives slightly better agreement with the measured ground state distribution, in particular at small angles.

In a microscopic approach, folding model calculations using the nucleon-nucleon potential proposed by Jeukenne, Lejeune and Mahaux (JLM) [14] have had success at describing nucleon nucleus scattering, provided the imaginary potential is adjusted by a normalization factor typically around 0.8 [16]. The present elastic scattering data is also well reproduced by a folding model calculation (dotted line in Fig. 2), which folds nuclear densities with the JLM nucleon-nucleon potential. The densities were calculated in a shell model using the full  $0f_{7/2}$  space [15,17]. The analysis of the elastic scattering, using both macroscopic and microscopic potentials, reveals no appreciable deviation, in the angular range studied, with respect to the systematics obtained for stable nuclei.

The cross section of the  $2_1^+$  state was obtained using two methods. First, the  $2_1^+$  state was selected in the excitation energy spectrum, and the angular distribution was obtained, Fig. 2(a), in the range where the ground state and  $2_1^+$  distributions are resolved ( $24^\circ$ - $39^\circ$ ). This process may be slightly inaccurate because of small overlap of the ground state with the  $2_1^+$  distribution, see insert of Fig. 1(b); however the shape of the inelastic scattering distribution can be compared on Fig. 2(a) with the coupled channel ECIS calculation using the  $\beta_2$  value extracted below. The shape of the experimental angular distribution is in full agreement with the calculation.

In order to extract the value of  $\beta_2$ , Gaussian distributions were fit to the ground state, the  $2_1^+$  state, and the very low background as shown in the insert of Fig. 1(b), for three angular bins. and the  $\chi^2$  of the coupled-channels prediction for the  $2_1^+$  state was minimized to obtain the measured deformation parameter. The extracted cross sections and the calculations are shown in Fig. 2(b). Using the Becchetti-Greenlees parameterization (dashed line) [13] the cross sections extracted from the Gaussian fits yield  $\beta_2=0.35 \pm 0.04$  while the  $^{40}\text{Ar}$  optical parameters of ref. [10] (solid line) give  $\beta_2=0.36 \pm 0.04$ . This shows that the extraction of the  $\beta_2$  value is essentially potential independent, provided that the elastic scattering is well

reproduced. In the following we will adopt the value  $\beta_2 = 0.35$ .

The  $M_n/M_p$  ratio was calculated using the formula derived in ref. [5]:

$$\frac{M_n}{M_p} = \frac{b_p}{b_n} \left( \frac{\delta}{\delta_{e.m.}} \left( 1 + \frac{b_n N}{b_p Z} \right) - 1 \right).$$

where  $b_p$  and  $b_n$  are the interaction strengths of protons with protons and neutrons respectively,  $\delta$  is the deformation length from (p,p') and  $\delta_{e.m.}$  is the electromagnetic deformation length ( $\delta = \beta_2 r_0 A^{1/3}$ ). An  $r_0$  value of 1.17fm corresponding to the optical parameters of the Bechetti-Greenlees systematics was used for (p,p') scattering, while  $r_0 = 1.20$ fm was taken for electromagnetic excitation. The  $b_p$  and  $b_n$  values were taken as 0.3 and 0.7, respectively [6]. The  $\beta_2$  for electromagnetic excitation is  $0.25 \pm 0.016$  taken from the Coulomb excitation measurement of ref. [4]. This yields  $M_n/M_p = 2.0 \pm 0.4$  for the  $2_1^+$  state in  $^{38}\text{S}$ , and thus  $M_n/M_p = (1.5 \pm 0.3)N/Z$ , which is incompatible with the value of  $N/Z$  expected for a pure isoscalar collective excitation.

It is interesting to observe the trend of  $\beta_2$  and  $M_n/M_p$  values for the  $2_1^+$  state as a function of neutron number in the sulfur isotopes, which are displayed in table 1. The  $M_n/M_p$  values were calculated from the experimental  $\beta_2$  values for low energy ( $E < 50$  MeV) proton scattering and electromagnetic excitation using the procedure described above. One should first note the very low  $\beta_2$  values and high excitation energy of the  $2_1^+$  state in  $^{36}\text{S}$ , as well as the  $M_n/M_p$  value compatible with  $N/Z$ . Therefore  $^{36}\text{S}$  exhibits features akin to those of a well closed nucleus. When moving away from  $^{36}\text{S}$ , the measured  $\beta_2$  values increase and a large difference in  $M_n/M_p$  values is observed between  $^{32}\text{S}$  and  $^{38}\text{S}$ , showing a rapid change of the structure as a function of neutron number. The large  $M_n/M_p$  value for  $^{38}\text{S}$  can be qualitatively understood by considering the  $^{38}\text{S}$  nucleus as a  $^{36}\text{S}$  core plus two valence neutrons. In this case, the two neutrons drive the oscillation and the core polarization is not sufficient to restore the isoscalar character of the excitation. It would be interesting to study the case of  $^{30}\text{S}$ , in order to confirm the slightly decreasing trend observed for  $M_n/M_p$  with decreasing neutron number.

We have measured extensive angular distributions for elastic scattering and, for the



first time, for inelastic scattering of protons on an unstable nucleus produced by projectile fragmentation, in this case  $^{38}\text{S}$ . The use of a large array of silicon-strip telescopes to measure recoiling protons in inverse kinematics proved to be a powerful and straightforward method to measure excitation energy spectra and angular distributions for unstable nuclei with reasonable resolution and low background. Elastic scattering was analyzed both in terms of macroscopic and microscopic potentials. The measured inelastic cross section for the first  $2_1^+$  state yields  $\beta_2 = 0.35 \pm 0.04$ . A comparison with electromagnetic excitation allows us to extract  $M_n/M_p = (1.5 \pm 0.3)N/Z$ , indicating a significant isovector contribution to the  $2_1^+$  state. This suggests that  $^{38}\text{S}$  can be considered as a  $^{36}\text{S}$  core and two valence neutrons. It would now be interesting to investigate the persistence of such a structure for larger neutron numbers, for which the neutron skin effects may be more pronounced. In this aim, a similar experiment has recently been performed for  $^{40}\text{S}$ .

We thank Alex Brown for numerous discussions and Nicolas Alamanos for his help in performing the folding model calculations. This work was partially supported by the National Science Foundation under grants Nos. PHY-9528844, PHY-9523974 and PHY-9403666.

## REFERENCES

- \* Present address TUNL, Duke University, Durham, NC 27708.
- † Present address Cyclotron Institute, Texas A&M University, College Station, TX 77843.
- ‡ Present address Allegheny College, Meadville, Pa 16335.
- § Present address Ludwig-Maximilian-Universität, München, Germany.
- [1] T. R. Werner *et al.*, Nucl. Phys A **597** (1996) 327.; T. R. Werner *et al.*, Phys Lett. B **335** (1994) 259.
- [2] T. Glasmacher *et al.*, preprint MSUCL-1084 (1997) and Phys. Lett. B (to be published).
- [3] O. Sorlin *et al.*, Nucl. Phys. **A583** (1995) 763.
- [4] H. Scheit, *et al.*, Phys. Rev. Lett. **77** (1996) 3967.
- [5] A.M. Bernstein, V.R. Brown, and V.A. Madsen, Comments Nucl. Part. Phys. **11** (1983) 203.
- [6] M.A. Kennedy, P.D. Cottle and K.W. Kemper, Phys. Rev. C **46** (1992) 1811.
- [7] G. Kraus *et al.*, Phys. Rev. Lett **73** (1994) 1773.
- [8] B.M. Sherrill *et al.*, Nucl. Instrum. Meth. **B70**, 298 (1992).
- [9] J. Raynal, Phys. Rev. C **23** (1981) 2571.
- [10] E. Fabrici *et al.*, Phys. Rev. C **21** (1980) 830.
- [11] R. De Leo *et al.*, Phys. Rev. C **31** (1985) 362.
- [12] P.M. Endt, Nucl. Phys. A **521** (1990) 599.
- [13] F.D. Becchetti Jr., and G.W. Greenlees, Phys. Rev. **182** (1969) 1190.
- [14] J.- P. Jeukenne *et al.*, Phys. Rev. C **16** (1977) 80.

- [15] B.A. Brown, Private communication.
- [16] F. Petrovich *et al.*, Nucl. Phys. A**563** (1993) 387.
- [17] W.A. Richter *et al.*, Nucl. Phys. A**577** (1994) 585.
- [18] S. Raman *et al.*, Atomic Data and Nuclear Data Tables **36** (1987) 1.
- [19] R. de Leo *et al.*, Nuovo Cimento **59A** (1980) 101.
- [20] R. Alarcon *et al.*, Phys. Rev. C**31** (1985) 697.
- [21] A. Hogenbirk *et al.*, Nucl. Phys. A**516** (1990) 205.

## FIGURES

FIG. 1. (a) Energy vs. angle scatterplot for recoiling protons from 40A MeV  $^{40}\text{Ar}(\text{p},\text{p}')$  in inverse kinematics. Insert: the excitation energy spectrum for the center of mass angular range of  $30.5^\circ$ - $31.5^\circ$ . The solid lines correspond to Gaussian fits (see text). (b) Same as (a) for 39A MeV  $^{38}\text{S}(\text{p},\text{p}')$ . Insert: the excitation energy spectrum for the center of mass angular range of  $27^\circ$ - $30^\circ$ . The solid lines correspond to Gaussian fits (see text).

FIG. 2. (a) Angular distributions for the ground state and the  $2_1^+$  state in the  $^{38}\text{S}(\text{p},\text{p}')$  reaction at 39A MeV, obtained by projecting the contents of contours (see text). (b) The elastic scattering data and calculations are the same as in (a). The  $2^+$  data is obtained by the gaussian fit method (see text). In both (a) and (b) the calculations are coded as follows ; dashed line: coupled channel calculation with Becchetti-Greenlees potential; solid line: coupled channel calculation with  $^{40}\text{Ar}(\text{p},\text{p}')$  potential; dotted line: folding model calculation; for details see text.

TABLES

TABLE I. Compilation of  $2_1^+$  states for sulfur isotopes. Energies and  $\beta_2(em)$  values are from ref. [18].  $\beta_2(p, p')$  values are from refs. [19] ( $^{32}\text{S}$ ), [20] ( $^{34}\text{S}$ ), [21] ( $^{36}\text{S}$ ) and from this work ( $^{38}\text{S}$ ).

	E (MeV)	$\beta_2(p, p')$	$\beta_2(em)$	$(M_n/M_p)/(N/Z)$
$^{32}\text{S}$	2.23	0.28	0.31	0.84
$^{34}\text{S}$	2.12	0.28	0.25	1.12
$^{36}\text{S}$	3.29	0.18	0.16	1.12
$^{38}\text{S}$	1.29	0.35	0.25	1.5

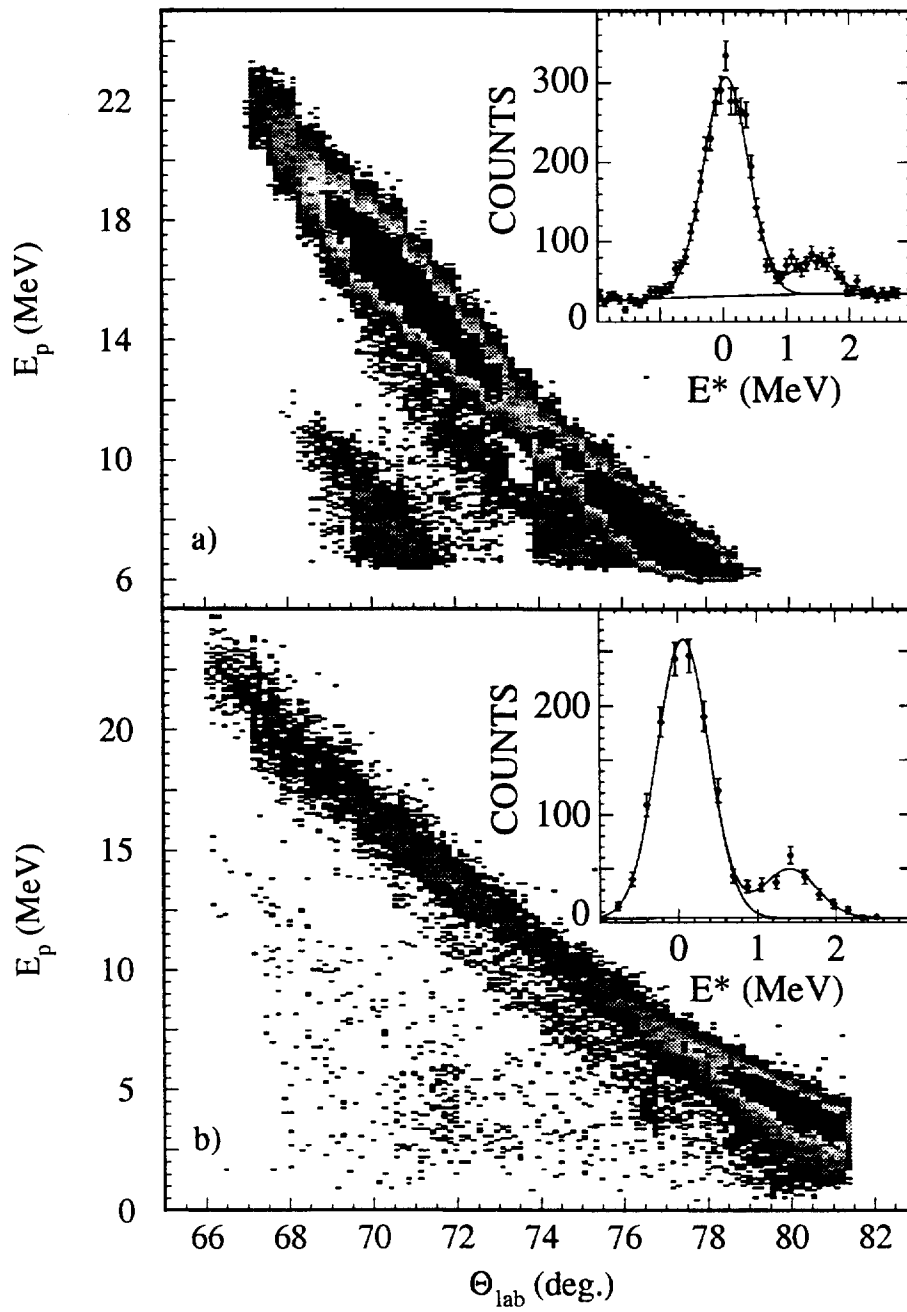


Fig. 1

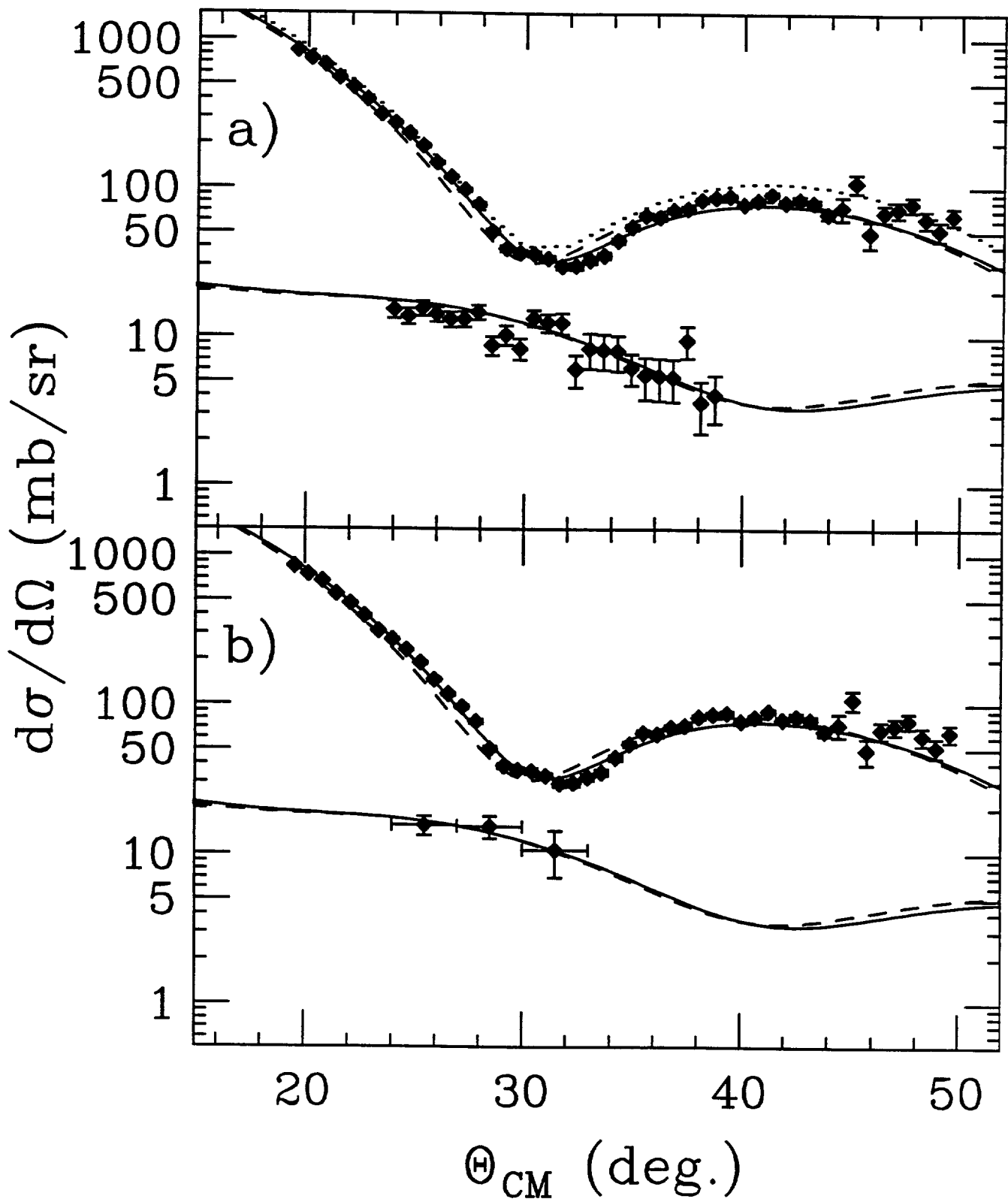


Fig. 2